SERBIAN JOURNAL OF ELECTRICAL ENGINEERING
Vol. 1, No. 3, November 2004, 69 - 77

Self-Consistent Treatment of V-Groove Quantum Wire Band Structure in Nonparabolic Approximation

Jasna V. Crnjanski [1], Dejan M. Gvozdic[2]

Abstract: The self-consistent nonparabolic calculation of a V-groove-quantum-wire (V-QWR) band structure is presented. A comparison with the parabolic flat-band model of V-QWR shows that both, the self-consistency and the nonparabolicity shift subband edges, in some cases even in the opposite directions. These shifts indicate that for an accurate description of intersubband absorption, both effects have to be taken into the account.

Keywords: V-QWR, Band structure, Self-consistent procedure, Nonparabolic approximation, Resonance.

1 Introduction

A lot of effort has been invested recently to enhance the properties of low-dimensional semiconductor devices by reducing the degrees of freedom of carriers. The development of quantum-well (QW) structures, in which electrons or holes are confined to two dimensions, has lead to a vast range of applications. It is expected that the further increase of confinement degree might open new possibilities and more advanced applications as well as significant improvements of present state-of-the-art devices. Predicted improvements include reduced threshold currents of lasers [1], approaching zero-threshold, improved temperature sensitivity [2], narrower line widths and increased differential gain, allowing higher-speed operation of devices at reduced power. In addition, a significant progress in the fabrication of devices based on intersubband transitions in quantum-confined structures, has initiated the intensive research of this phenomena in one-dimensional (1-D) [3,4] and zero-dimensional (0-D) [5] structures. These structures, in principle, can provide much sharper optical transitions than in QWs, due to singularities existing in their density of states [2].

In this paper, we investigate band structure of quantum wires (QWR) based on InGaAs/InP lattice-matched structure grown in InP V-grooves. In addition, we consider the influence of band structure on intersubband transitions in these structures. It has been proved that V-shaped quantum wires (V-QWR), can be easily fabricated [6], while their size can be successfully controlled by the anisotropic etching [6]. However, their ge-

[1] Faculty of Electrical Engineering, University of Belgrade, P.O. Box 35-54, Serbia, email: jafa@etf.bg.ac.yu
[2] Faculty of Electrical Engineering, University of Belgrade, P.O. Box 35-54, Serbia
Present address: KTH The Royal Institute of Technology, Laboratory of Optics, Photonics and Quantum Electronics, Sweden

ometry and the lack of symmetry make them heavily accessible for less-demanding theoretical means, as in case of QWRs with cylindrical [7] or rectangular cross-section [8]. In order to derive as much as possible realistic conclusions about their electronic structure, it is necessary to consider V-QWR as it is actually measured by atomic-force micrography [6]. In addition, we take into account influence of the barrier doping, providing necessary carriers for optical transitions within the conduction band. Since the mixing of heavy and light holes occurs even at the Γ point of the valence band, nonparabolicity might play significant role on band profile in such structures. Therefore, we include this effect in our calculation by Kane's relation [9,4], having in mind that the more exact calculation would require treatment based on the 8×8 Luttinger-Kohn Hamiltonian.

2 Theoretical Analysis

We consider an InP/InGaAs V-QWR with the cross section profile (in lateral direction) described by the relation as

$$y = \sqrt{K_l^2 - d^2} - \sqrt{K_l^2 - x^2}\ , \tag{1}$$

where x and y represent coordinates in the cross section plane, $2d$ is the width of the V-QWR, and K_l is the parameter specifically chosen for fitting upper and lower boundary between the well (InGaAs) and the bulk (InP) [9] (Fig.1).

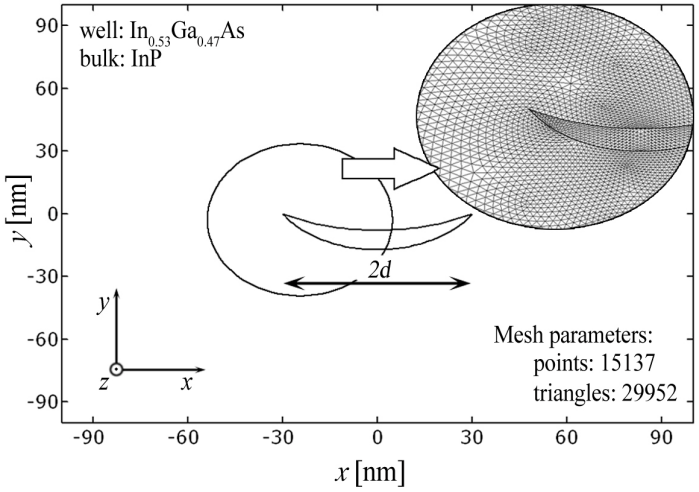

Fig. 1 - *Profile of V-QWR and domain of self-consistent solving. Detail view of mesh distribution.*

The electronic structure of the conduction band is determinated from the Schrödinger equation,

$$\frac{\hbar^2}{2}\nabla_{xy}\left(\frac{1}{m^*(x,y)}\nabla_{xy}\right)\chi(x,y)+\left(E-\frac{\hbar^2 k_z^2}{2m^*(x,y)}-E_c(x,y)\right)\chi(x,y)=0\,, \quad (2)$$

where $\chi(x,y)$ is the envelope wave function of the total electron wave function in the conduction band, $\psi(x,y,z)=\chi(x,y)\exp[\mathrm{i}k_z z]$, while k_z is the wave vector in the z direction (Fig.1). The potential in the Schrödinger equation is defined by the bottom of the conduction band profile $E_c(x,y)$. Due to the barrier doping with donors (concentration $N_d=10^{16}\,\mathrm{cm}^{-3}$), the $E_c(x,y)$ profile is defined with the conduction-band discontinuity $\Delta E_c=250$ meV, as well as with the potential $\varphi(x,y)$, which results from the electrons in the structure and ionised donors $N_d{}^+$ in the barrier. This potential can be calculated by solving 2D-Poisson and 2D-Schrödinger equations self-consistently. The Poisson equation is given by:

$$\nabla[\varepsilon(x,y)\nabla\varphi(x,y)]=-q\cdot\left(N_d^+-n(x,y)\right), \quad (3)$$

where $\varepsilon(x,y)$ represents the spatial dependence of static dielectric permeability, $\varphi(x,y)$ spatial dependence of potential, $N_d{}^+$ concentration of ionised donors in the bulk material, and $n(x,y)$ is electron concentration, which is separately defined for the well and the bulk region:

$$n(x,y)=\begin{Bmatrix} n_w(x,y), & \text{for } (x,y)\in D_w \\ n_w(x,y)+n_b(x,y), & \text{for } (x,y)\in D_b \end{Bmatrix}. \quad (4)$$

In Eq. (4)

$$n_w(x,y)=\frac{2}{\pi}\sum_p\left|\chi_p(x,y)\right|^2\int_0^{+\infty}\frac{dk_z}{1+\exp\left[\dfrac{E_p(k_z)-F_n}{k_bT}\right]} \quad (5)$$

represents electron concentration in the well. In Eq. (5), E_p is p-subband energy, while F_n is energy of Fermi level. On the other hand, the electron concentration in bulk is given by:

$$n_b(x,y)=N_c\cdot F_{1/2}\left(\frac{F_n+q\cdot\varphi(x,y)}{k_bT}\right), \quad (6)$$

where the effective conduction band density of states in barrier is $N_c=5.7\times10^{17}\,\mathrm{cm}^{-3}$ and $F_{1/2}$ is Fermi integral. Ionised donors concentration is given by the relation

$$N_d^+ = N_d - \frac{N_d}{1+\frac{1}{2}\exp\left[\frac{E_d - F_n - q\cdot\varphi(x,y)}{k_b T}\right]}, \tag{7}$$

where E_d is donor energy level. This level is shifted $5.7\,\text{meV}$ below the bottom of conduction band.

From Eq. (3), Eq. (6) and Eq. (7) can be concluded that the Poisson equation is a non-linear partial differential equation, and is solved entirely in every iteration of the self-consistent procedure, what represents great relief in aspect of number of iterations. It should be noted that adopted method does not rely on assumptions of the total depletion approximation, nor it assumes actual profile of the depletion region. Therefore, the method is well applicable for vast range of doping concentrations and temperatures. The Fermi level in respect to the bottom of conduction band, at the edges of domain, is calculated from the condition of the global electrical neutrality.

The convergence of this procedure is accomplished by calculating potential in $(i+1)$-th iteration, according to the relation:

$$\varphi_{i+1}(x,y) = (u_i(x,y) + \varphi_i(x,y) + \varphi_{i-1}(x,y) + \varphi_{i-2}(x,y))/4\,, \tag{8}$$

where $u_i(x,y)$ is potential at the end of iteration i, and $\varphi_i(x,y), \varphi_{i-1}(x,y)$ and $\varphi_{i-2}(x,y)$ are potentials at the beginning of i-th, $(i-1)$-th and $(i-2)$-th iterations, respectively.

Previously presented self-consistent procedure can also be applied to the nonparabolic approximation very efficiently. The nonparabolicity is taken into account by Kane's relation [9,4], where effective mass becomes energy dependent. Using corrected value for the effective mass, new energy E_p is calculated. This procedure is being repeated, in particular for every energy level and wave vector of interest, altogether three times, since the convergence is very fast [9].

Finally, the potential, calculated in $(i+1)$-th iteration, determines the profile of conduction band $E_c(x,y)$, according to the relation:

$$n(x,y) = \begin{Bmatrix} -q\cdot\varphi_i(x,y) - \Delta E_c, & \text{for } (x,y)\in D_w \\ -q\cdot\varphi_i(x,y), & \text{for } (x,y)\in D_b \end{Bmatrix}, \tag{9}$$

which is again used for solving the Schrödinger equation.

The self-consistent procedure is based on the finite element method with nonuniform mesh of triangular elements (Fig.1). For our numerical example, compromise between accuracy and processor time needed for the calculation is obtained for something less than 30 000 triangular elements.

3 Results and Discussion

The self-consistent approach proposed in our paper allows for fast convergence of the coupled Poisson-Schrödinger equation. This is demonstrated in Fig.2, showing the

absolute value of the potential maximum for different stages of an iterative process. The initial step is calculated parabolic band structure of V-QWR, without self-consistency (P) [9]. The potential is due to electron's charge inside the well and its screening by positive ionised donors still doesn't occur, since they are not revealed in this stage. After five iterations, when ionised donors become revealed and region in vicinity depilated, deviation from the final potential in self-consistent-parabolic approximation (SCP) is rather small (less than $10\,\text{meV}$) and after 10 iterations is almost negligible. In order to prepare the procedure for self-consistent-nonparabolic approximation (SCN), we continue with SCP iterations up to 16, when the subsequent deviation of bound state's eigenenergy is less than $1\,\text{meV}$. Then we introduce the energy-dependent effective mass in our calculation and the procedure ends after six iterations, which in the total includes 22 iterations.

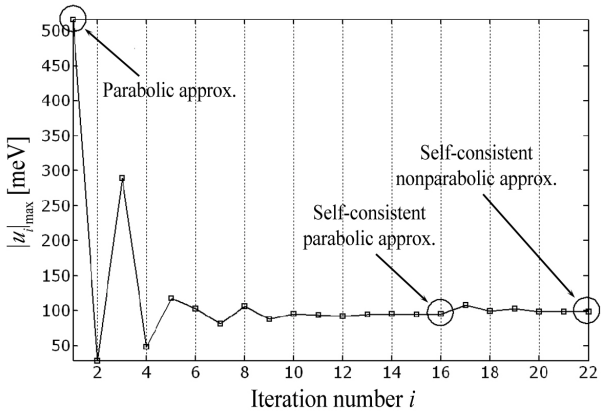

Fig. 2 - *The peak value of the potential u_i versus self-consistent iteration.*

Fig.3 shows calculated profile of the potential (a), electron concentration in the well (b), and the conduction band profile for doping concentration $N_d = 10^{16}\,\text{cm}^{-3}$, after 22 iterations. The potential effectively shifts the bottom of the well for about 40meV, although the total shift is about $100\,\text{meV}$ (see Fig.3a and the maximum of the potential). The barrier bottom in vicinity of the well is shifted about $60\,\text{meV}$ from its original value and represents the rest of potential shift. These shifts give possibility for appearance of resonance (subbands No.8 to No.12). An additional reason for that is the fact that the confinement after the self-consistent treatment is not isotropic anymore, since it is weakened in the *x*-direction (Fig.3c). However, the Fermi level is far away from those states ($F_n = -103.86$ meV) and its effect on carrier concentration cannot be noticed (Fig.3b). The maximum carrier concentration in the well is $n_w = 7\times10^{17}\,\text{cm}^{-3}$ and it occurs in the vicinity of tips of the V-QWR. In this region wave functions exhibit the largest peaks as a

consequence of an effectively parabolic-well potential in the wire [9], which generally speaking, might be affected by the shift of the potential in the centre of the well.

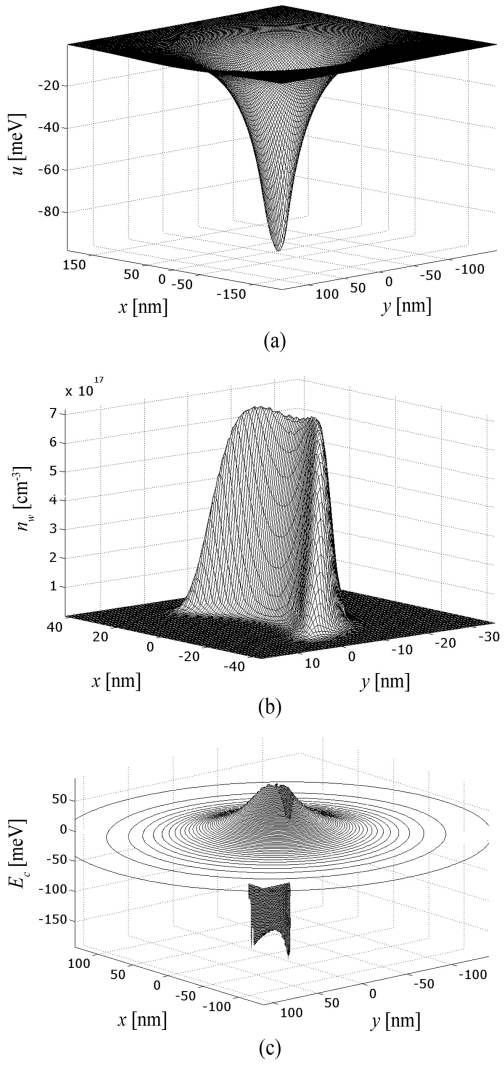

Fig. 3 - *The final profile of potential (a), electron concentration in the well (b), and the conduction band profile (c) for doping concentration* $N_d = 10^{16}$ cm .

In order to demonstrate the influence of the barrier doping and the nonparabolicity on the conduction band structure of V-QWRs, we show band structure versus free wave

vector k_z (Fig.4) in P and SCN approximations. Although the effect of the nonparabolicity becomes noticeable for larger values of k_z, it also affects the Γ point.

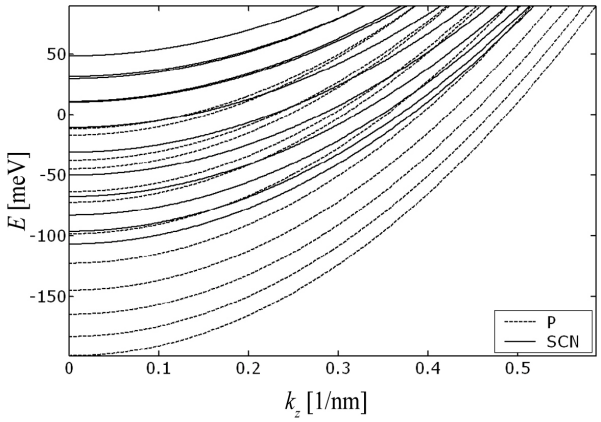

Fig. 4 - *The band structure of V-QWR conduction band for parabolic non-self-consistent and nonparabolic self-consistent calculation.*

The total deviation of P approximation from realistic SCN approximation is shown in Fig.5a, demonstrating the influence of both effects, the self-consistency and the nonaparbolicity. To distinguish particular contribution of each of them, we determine the differences of calculated eigenenergies in P and SCP approximation (Fig.5b), and SCP and SCN approximation on the other side (Fig.5c). Fig.5b clearly shows that the self-consistency affects all bound states, but not to the same extent. The most pronounced shift can be observed for the ground state, while for others it decreases up to the 7-th state. Since for higher, resonant states, the nodes of wave function extend in the direction of stronger confinement, the same order of shifts doesn't apply anymore. It can be seen that bending is negligible in this case, even when the penetration of wave function into the barrier is more pronounced due to the self-consistent potential. Although the absolute shift due to the self-consistency is large, the range of shifts is less than $20\,\mathrm{meV}$ (from $-70\,\mathrm{meV}$ to $-90\,\mathrm{meV}$). The comparison of SCP and SCN approximation exhibits almost the same range of relative shift (Fig.5c). However, the absolute shift in this case is much smaller (no more than $15\,\mathrm{meV}$). The bending of the difference $E_{\mathrm{SCP}} - E_{\mathrm{SCN}}$ versus k_z is a E consequence of the nonparabolicity. Due to different signs of subbands shifts, the nonparabolicity might affect the absorption spectrum [4] nearly to same extent as the self-consistency. This can be seen in Fig.5a, where the range of the total subband shift varies from $-50\,\mathrm{meV}$ to $-90\,\mathrm{meV}$. The bending itself has no large influence on the absorption spectrum or its line width, since separation between subbands remains more or less fixed as in the parabolic case.

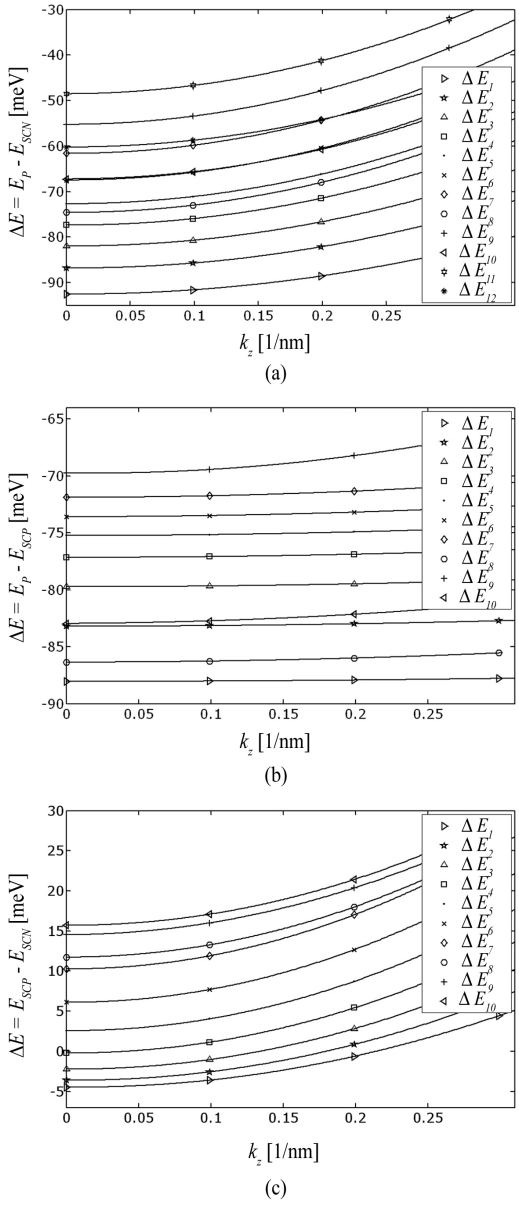

Fig. 5 - *Deviation of subband energies from nonparabolic self-consistent values for parabolic non-self-consistent (a) and parabolic self-consistent calculation (c). Same for parabolic non-self-consistent and self-consistent case (b).*

4 Conclusions

We have performed self-consistent calculation of a realistic V-groove QWR band structure in a parabolic and nonparabolic approximation. Our method allows us to calculate accurately the band structure as well as all the relevant quantities beyond limitations of the total depletion approximation. Comparison with the parabolic, flat-band electronic structure of V-QWR shows, that either the self-consistency or the nonparabolicity affect the subband structure significantly. Although the absolute shift of bound states due to the self-consistency is more pronounced than in the case of nonparabolicity, it appears that their cumulative impact on the band structure, and consequently, the intersubband absorption spectrum, might be important.

5 References

[1] D. M. Gvozdi}, N. M. Nenadovi}, A. Schlachetzki: Gain and Threshold-Current Calculation of V-Groove Quantum-Wire InGaAs-InP Laser, IEEE J. of Quantum Electron., Vol. 38, No. 12, 2002, pp. 1565-1579.

[2] D. M. Gvozdi}, A. Schlachetzki: Influence of Temperature and Optical Confinement on Threshold Current of an InGaAs/InP Quantum Wire Laser, IEEE J. of Selected Topics in Quantum Electron., Vol. 9, No. 3, 2003, pp. 732-735.

[3] Y. Fu, M. Willander, X-Q. Liu, W. Lu, S. C. Shen, H. H. Tan, C. Jagadish, J. Zou, D. J. H. Cockayne: Optical transition in infrared photodetector based on V-groove $Al_{0.5}Ga_{0.5}As$/GaAs multiple quantum wire, J. of Appl. Phys., Vol. 89, No. 4, 2001, pp. 2351-2356.

[4] D. M. Gvozdi}, A. Schlachetzki: Intersubband absorption in V-groove quantum wires, J. Appl. Phys., Vol. 94, No. 8, 2003, pp. 5049-5052.

[5] S. Krishna, P. Bhattacharya, P. J. McCann, K. Namjou: Room-temperature long wavelength ($\lambda = 13.3\mu m$) unipolar quantum dot intersubband laser, Electronics Letters, Vol. 36, No. 18, 2000, pp. 1550-1551.

[6] T. Schrimpf, P. Bönsch, D. Wüllner, H.-H. Wehmann, A. Schlachetzki, F. Bertram, T. Riemann, J. Chirsten: InGaAs quantum wires and wells on V-grooved InP substrates, J. Appl. Phys., Vol. 86, No. 9, 1999, pp. 5207-5214.

[7] J. P. Leburton: Intersubband stimulated emission and optical gain by «phonon pumping» in quantum wires, J. Appl. Phys., Vol. 74, No. 2, pp. 1417-1420, July 1993.

[8] M. Tadi}, Z. Ikoni}: Self-consistent electronic-structure calculation of rectangular modulation-doped GaAs/$Ga_{1-x}Al_xAs$ quantum wires, Phys. Rev. B, Vol. 50, No. 11, 1994, pp. 7680-7688.

[9] D. M. Gvozdi}, A. Schlachetzki: Electronic states in the conduction band of V-groove quantum wires, J. Appl. Phys., Vol. 92, No. 4, 2002, pp. 2023-2034.